JOURNAL OF PROPULSION AND POWER
Vol. 11, No. 6, November–December 1995

Dynamic Modeling of High-Speed Aircraft Generators During Forced Power Transfer Operation

A. A. Arkadan* and R. H. VanderHeiden†
Marquette University, Milwaukee, Wisconsin 53233-2286
and
J. F. Defenbaugh‡
Sundstrand Aerospace, Rockford, Illinois 61125-7002

A computer-aided method for modeling disturbances and to predict the reverse voltage across the rotating bridge rectifier of the field exciter due to the forced paralleling of out-of-phase high-speed salient pole ac generator-load systems is presented. The method is based on the use of state–space models in the time domain. The state–space model parameters are determined from finite element based nonlinear magnetic field solutions. Accordingly, the method accounts for saturation due to magnetic material nonlinearities and space harmonics effects due to machine geometry. The method is applied to predict the performance characteristics of two out-of-phase aircraft-type ac generators during forced power transfer (paralleling) operating conditions. This resulted in field winding, stator windings and damping circuits current, and voltage waveforms for the generator-load system. Predicted values of the induced field winding current and corresponding reverse voltages across the rotating diode rectifier bridge of the field excitors are shown to be in close agreement with test results.

Introduction

TO avoid severe shocks when connecting a generator to an infinite bus, or paralleling it with one or more generators, a synchronizing procedure must be followed before closing the circuit breakers.[1,2] Among other things, the paralleling of a generator to a system requires adjusting its speed, frequency, terminal voltages, phase sequence, and phase angle to conform to those values existing in the system where it is to be connected at the instant the circuit breakers are closed. However, in some cases power transfer or paralleling is forced between two phase-displaced generators. That is, the circuit breakers that parallel the two generators are closed when there is a difference in the phase of the two sets of the three-phase voltages.

Forced power transfer (FPT), or paralleling with a phase difference between two generators, can take place in aerospace applications due to controller restrictions. In such applications, paralleling can occur between two integrated drive generators (IDGs) (Fig. 1), an IDG and an auxiliary power unit (APU) generator, or an IDG and ground power. In the case of the ground power or APU generator, there are multiple controllers involved that would have to be coordinated to minimize the difference between the terminal voltage phase angles of the two systems before paralleling. Additionally, once the decision is made to parallel, the command is relayed to the contactor control unit adding delay time between the decision and implementation. Another cause for paralleling without phase coordination is during some type of ground fault or communication failure when the contactor is closed without the ability or time to coordinate the phase relationship.

During FPT in a system, very high negative field current circulates back through the shunt resistor of the generator exciter, which results in a reverse voltage across the rectifier bridge diodes (Fig. 1). If the value of the reverse voltage exceeds the rated reverse voltage of the bridge rectifier diodes, the diodes fail. Accordingly, the prediction of the performance characteristics during such conditions is essential for proper rating of the system components, to avoid failures, and to increase the system reliability.

The modeling approach for investigating disturbances due to the forced paralleling of out-of-phase high-speed salient pole ac generator systems feeding isolated loads is presented. The method involves the use of state–space models in the natural *abc* frame of reference and the determination of the machine winding inductances from magnetic field solutions to account for magnetic saturation as well as space harmonics effects.[3,4] This is in contrast to models in the *d-q* frame of Refs. 5 and 6, which involve the assumption of sinusoidally distributed magnetomotive forces (mmf) and flux linkages. Such *d-q* models require the use of empirical or semiempirical techniques to account for saturation and space harmonic effects.

The case study is performed on the system of Fig. 1. Although this system involves two generators, the modeling approach is valid for multigenerator systems under different operating conditions.

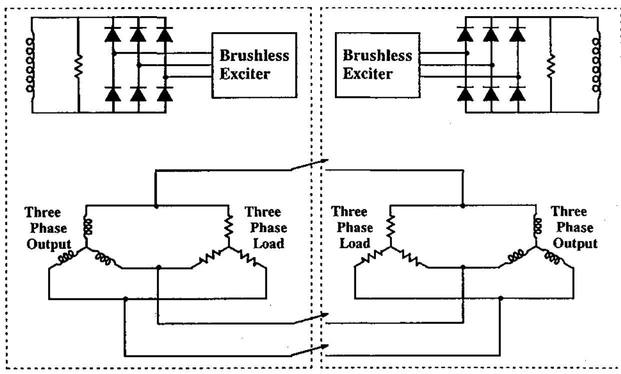

Fig. 1 System schematic.

Received Aug. 1, 1994; revision received Feb. 6, 1995; accepted for publication March 1, 1995.
*Associate Professor, Electrical and Computer Engineering.
†Research Assistant, Electrical and Computer Engineering.
‡Senior Research Engineer, Applied Research.

System–Model Description

Consider the system of Fig. 1. It is assumed that each of the two generators is supplying power to a three-phase Y-connected load before the onset of the paralleling operation. The two machines considered in this investigation have identical ratings and geometries. The two machines are identical in that each is a three-phase, field wound, salient pole ac generator with brushless exciter, rated at 90 kVA, 208 V, and 400 Hz. The stator 48 slots house the generator three-phase two-layer armature windings. The rotor four-pole structure includes the main field coil that is formed by four series connected windings. Further, it includes 20 damper bars that are embedded in the four pole faces. The brushless exciter system for each generator includes a rotating diode rectifier bridge that supplies the field winding through a shunt resistor.

The differential equations used to model the dynamic performance of electrical machines in general, and ac machines in particular, are derived from the interaction between the armature windings, field, and damping circuits.

For the case studied, each machine is represented by six windings, where the windings a, b, and c represent the armature three phases, the winding f represents the rotor field winding, and the shorted windings kd and kq represent the squirrel cage-type damper bars. Accordingly, if one of the n generators is denoted as generator i, one can relate the terminal voltages in terms of the flux linkages using a compact matrix notation as

$$\underline{V}^i = \underline{R}^i_g \underline{I}^i + \frac{\mathrm{d}}{\mathrm{d}t}\underline{\Lambda}^i_g \tag{1}$$

where the flux linkage $\underline{\Lambda}^i_g$ is expressed in terms self and mutual apparent inductance and currents associated with all the coupled windings. Further, if the load of generator i has a per phase resistance r^i_l and inductance L^i_l, the armature terminal voltages of this generator can be expressed as

$$\underline{V}^i_{abc} = \underline{R}^i_L \underline{I}^i_{abc} + \underline{L}^i_L \frac{\mathrm{d}}{\mathrm{d}t}\underline{I}^i_{abc} \tag{2}$$

In the case of a pure resistive load, the differential equations governing the performance of the system of Fig. 1 during FPT operation is derived from the expressions in Eqs. (1) and (2) and is given by Eq. (3):

$$\begin{bmatrix} 0 \\ 0 \\ 0 \\ v^1_f \\ 0 \\ 0 \\ 0 \\ 0 \\ 0 \\ v^2_f \\ 0 \\ 0 \end{bmatrix} = \begin{bmatrix} r_s+r_l/2 & 0 & 0 & 0 & 0 & 0 & r_l/2 & 0 & 0 & 0 & 0 & 0 \\ 0 & r_s+r_l/2 & 0 & 0 & 0 & 0 & 0 & r_l/2 & 0 & 0 & 0 & 0 \\ 0 & 0 & r_s+r_l/2 & 0 & 0 & 0 & 0 & 0 & r_l/2 & 0 & 0 & 0 \\ 0 & 0 & 0 & r_f & 0 & 0 & 0 & 0 & 0 & 0 & 0 & 0 \\ 0 & 0 & 0 & 0 & r_{kd} & 0 & 0 & 0 & 0 & 0 & 0 & 0 \\ 0 & 0 & 0 & 0 & 0 & r_{kq} & 0 & 0 & 0 & 0 & 0 & 0 \\ r_l/2 & 0 & 0 & 0 & 0 & 0 & r_s+r_l/2 & 0 & 0 & 0 & 0 & 0 \\ 0 & r_l/2 & 0 & 0 & 0 & 0 & 0 & r_s+r_l/2 & 0 & 0 & 0 & 0 \\ 0 & 0 & r_l/2 & 0 & 0 & 0 & 0 & 0 & r_s+r_l/2 & 0 & 0 & 0 \\ 0 & 0 & 0 & 0 & 0 & 0 & 0 & 0 & 0 & r_f & 0 & 0 \\ 0 & 0 & 0 & 0 & 0 & 0 & 0 & 0 & 0 & 0 & r_{kd} & 0 \\ 0 & 0 & 0 & 0 & 0 & 0 & 0 & 0 & 0 & 0 & 0 & r_{kq} \end{bmatrix} \cdot \begin{bmatrix} i^1_a \\ i^1_b \\ i^1_c \\ i^1_f \\ i^1_{kd} \\ i^1_{kq} \\ i^2_a \\ i^2_b \\ i^2_c \\ i^2_f \\ i^2_{kd} \\ i^2_{kq} \end{bmatrix}$$

$$+ \frac{\mathrm{d}}{\mathrm{d}t}\left\{ \begin{bmatrix} L^1_{aa} & L^1_{ab} & L^1_{ac} & L^1_{af} & L^1_{akd} & L^1_{akq} & 0 & 0 & 0 & 0 & 0 & 0 \\ L^1_{ba} & L^1_{bb} & L^1_{bc} & L^1_{bf} & L^1_{bkd} & L^1_{bkq} & 0 & 0 & 0 & 0 & 0 & 0 \\ L^1_{ca} & L^1_{cb} & L^1_{cc} & L^1_{cf} & L^1_{ckd} & L^1_{ckq} & 0 & 0 & 0 & 0 & 0 & 0 \\ L^1_{fa} & L^1_{fb} & L^1_{fc} & L^1_{ff} & L^1_{fkd} & L^1_{fkq} & 0 & 0 & 0 & 0 & 0 & 0 \\ L^1_{kda} & L^1_{kdb} & L^1_{kdc} & L^1_{kdf} & L^1_{kdkd} & L^1_{kdkq} & 0 & 0 & 0 & 0 & 0 & 0 \\ L^1_{kqa} & L^1_{kqb} & L^1_{kqc} & L^1_{kqf} & L^1_{kqkd} & L^1_{kqkq} & 0 & 0 & 0 & 0 & 0 & 0 \\ 0 & 0 & 0 & 0 & 0 & 0 & L^2_{aa} & L^2_{ab} & L^2_{ac} & L^2_{af} & L^2_{akd} & L^2_{akq} \\ 0 & 0 & 0 & 0 & 0 & 0 & L^2_{ba} & L^2_{bb} & L^2_{bc} & L^2_{bf} & L^2_{bkd} & L^2_{bkq} \\ 0 & 0 & 0 & 0 & 0 & 0 & L^2_{ca} & L^2_{cb} & L^2_{cc} & L^2_{cf} & L^2_{ckd} & L^2_{ckq} \\ 0 & 0 & 0 & 0 & 0 & 0 & L^2_{fa} & L^2_{fb} & L^2_{fc} & L^2_{ff} & L^2_{fkd} & L^2_{fkq} \\ 0 & 0 & 0 & 0 & 0 & 0 & L^2_{kda} & L^2_{kdb} & L^2_{kdc} & L^2_{kdf} & L^2_{kdkd} & L^2_{kdkq} \\ 0 & 0 & 0 & 0 & 0 & 0 & L^2_{kqa} & L^2_{kqb} & L^2_{kqc} & L^2_{kqf} & L^2_{kqkd} & L^2_{kqkq} \end{bmatrix} \cdot \begin{bmatrix} i^1_a \\ i^1_b \\ i^1_c \\ i^1_f \\ i^1_{kd} \\ i^1_{kq} \\ i^2_a \\ i^2_b \\ i^2_c \\ i^2_f \\ i^2_{kd} \\ i^2_{kq} \end{bmatrix} \right\} \tag{3}$$

In the model, the notation v_a^1, v_b^1, and v_c^1 is used to represent the terminal voltages for phases a, b, and c, respectively, of generator no. 1. Similarly, the notation v_a^2, v_b^2, and v_c^2 is used for the phase voltages of generator no. 2.

In the case when n generators, each of which is feeding a Y-connected three-phase isolated resistive load $\underline{R}_L^i$, are paralleled, the terminal voltages have the relationship

$$\underline{V}_{abc}^1 = \underline{V}_{abc}^2 = \cdots = \underline{V}_{abc}^n \tag{4}$$

In addition, the terminal voltage $\underline{V}_{abc}^i$; $i = 1, 2, \ldots, n$ can be related to the new shared load as

$$\underline{V}_{abc}^i = \sum_{i=1}^{n} \left(\underline{R}_{eq} \underline{I}_{abc}^i \right) \tag{5}$$

Here, $\underline{R}_{eq}$ is given for the case of n generators supplying n paralleled loads, $\underline{R}_L^1$ through $\underline{R}_L^n$, respectively, as

$$\underline{R}_{eq} = \underline{R}_L^1 \| \underline{R}_L^2 \| \cdots \| \underline{R}_L^n \tag{6}$$

To study the FPT operation, it is considered that the two load systems are placed in parallel by closing the three circuit breakers (Fig. 1) at an instant where a phase shift α exists between the terminal voltages $\underline{V}_{abc}^1$ of generator 1, and the corresponding voltages $\underline{V}_{abc}^2$ of generator 2.

Further, in modeling the system, the two generators are considered identical, except for α that exists between corresponding phase voltages $\underline{V}_{abc}^1$ and $\underline{V}_{abc}^2$ at the commencement of the FPT operation. As can be appreciated from Eq. (3), the inductances are the main parameters of the state–space model. In this model, different inductance notation is used for each of the two generators. Superscript 1 is used to denote an inductance for generator no. 1 as L_{jk}^1, while superscript 2 is used to represent the corresponding inductance for generator no. 2 as L_{jk}^2. Here, the inductances are represented by Fourier-type expressions. These expressions are used to model the phase shift between the corresponding terminal voltages of the two generators.

For this study, where α exists between the terminal voltages $\underline{V}_{abc}^1$ and $\underline{V}_{abc}^2$, the inductances of generators nos. 1 and 2 are given by the following Fourier-type series expressions, respectively,

$$L_{jk}^1 = a_{jk,0}^1 + \sum_{h=1}^{NH} \{ a_{jk,h}^1 \cos[h(\theta)] + b_{jk,h}^1 \sin[h(\theta)] \} \tag{7}$$

$$L_{jk}^2 = a_{jk,0}^1 + \sum_{h=1}^{NH} \{ a_{jk,h}^1 \cos[h(\theta + \alpha)] + b_{jk,h}^1 \sin[h(\theta + \alpha)] \} \tag{8}$$

It should be noted here that since the two generators are identical, the Fourier series coefficients are identical for corresponding inductances, except that the expressions are shifted by an angle α with respect to each other. An energy and current perturbation approach applied to numerical magnetic field solutions provides the basis for the calculation of the machine self and mutual inductances in this work. The details of using this approach are given in Ref. 7 where the results are verified by comparison to test data. In the following, a description of the system experimental setup for measuring the effects of FPT on the rectifier bridge of the brushless exciter is presented. In addition, the simulation results are compared to test data for verification.

Experimental Setup

The test setup implemented in this work is given by the schematic diagram of Fig. 2. In this case, both generators are identical and are rated at 90 kVA, 208 V, and 400 Hz. In this test setup, generator no. 1 is using a brushless exciter. Meanwhile, the field exciter of generator no. 2 is modified by adding slip rings in order to get access to the rectifier bridge terminals. A description of the test setup is as follows:

1) The two generators are mounted on the same shaft, where the d axes of the main fields are aligned together, so that both generators are driven by the same prime mover and both have the same speed.

2) The phase angle between the two generators is adjusted by turning the stator cases with respect to each other. In other words, if the center of slot no. 1 in generators no. 1 and 2 are labeled as axis 1 and axis 2, respectively, a desired measurement mechanical angle β is established by rotating the stator cases to locate axis 1 at angle β from axis 2.

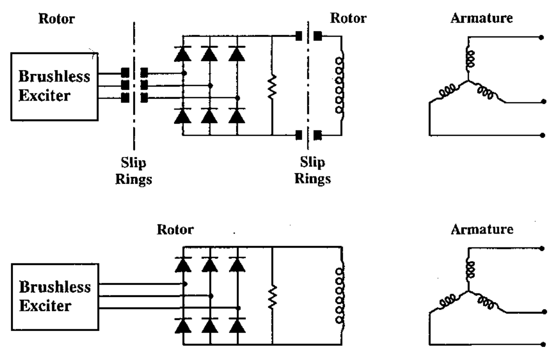

Fig. 2 Experimental system setup.

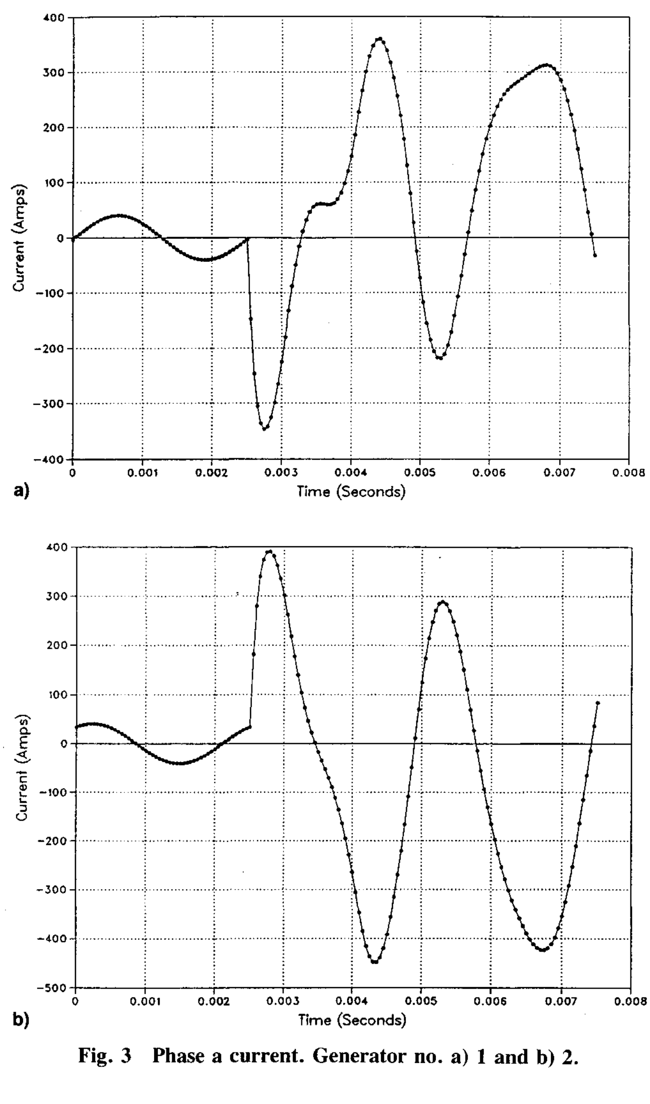

Fig. 3 Phase a current. Generator no. a) 1 and b) 2.

3) The two generator exciters are field controlled by two separate power supplies.

4) A digital storage scope is used to measure the field current and voltage.

5) The two generators are placed in parallel for a time interval set by a timer.

The results of this case study as obtained from simulations and measurements are given next.

System Performance Prediction and Verification

The results of implementing the approach outlined in this article are presented. First, the results of simulating this system for a phase shift $\alpha = 60$ deg electrical are given. Next, a summary of results obtained from repeating the analysis over a set of phase angles α, covering a range $20 \leq \alpha \leq 100$ deg electrical is presented.

The analysis of this system is performed over three ac cycles (7.5 ms). It is assumed that during the first cycle ($0 \leq t \leq 2.5$ ms) each of the generators is separately feeding a three-phase Y-connected resistive load rated at 10 kVA, unity power factor. At the beginning of the second cycle, $t = 2.5$ ms, the forced paralleling operation with $\alpha = 60$ deg is commenced. That is, the two loads are paralleled and are supplied by both generators simultaneously. This sequence of events was simulated over three ac cycles of operation in order to observe the effects of forced paralleling on the system performance and to compare the results to those found during normal operating conditions. The analysis was performed using Eq.

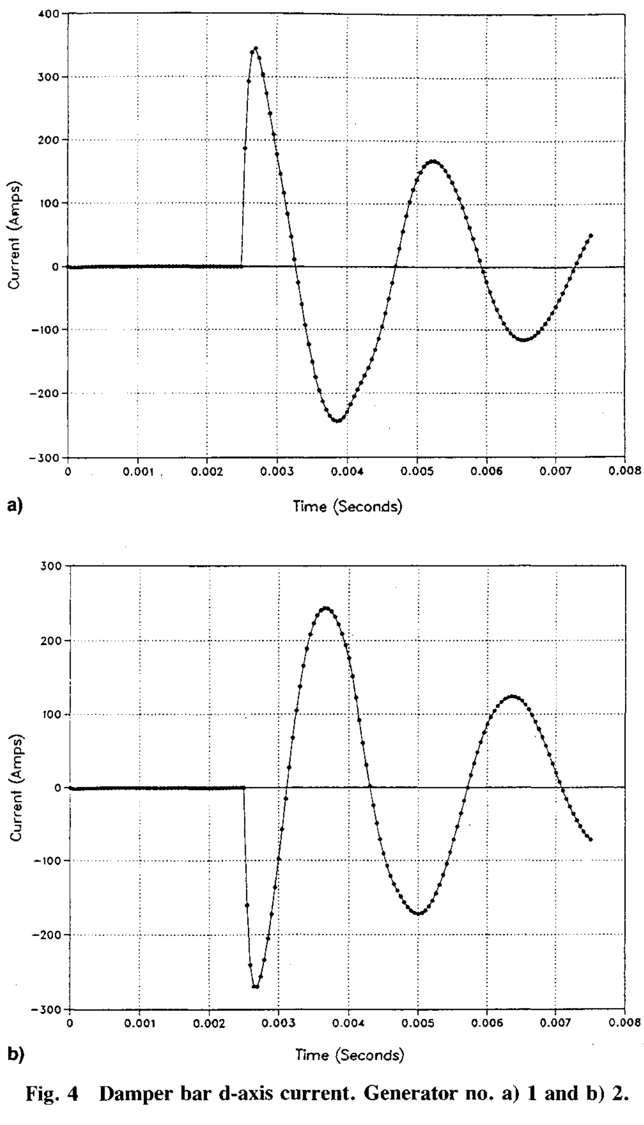

Fig. 4 Damper bar d-axis current. Generator no. a) 1 and b) 2.

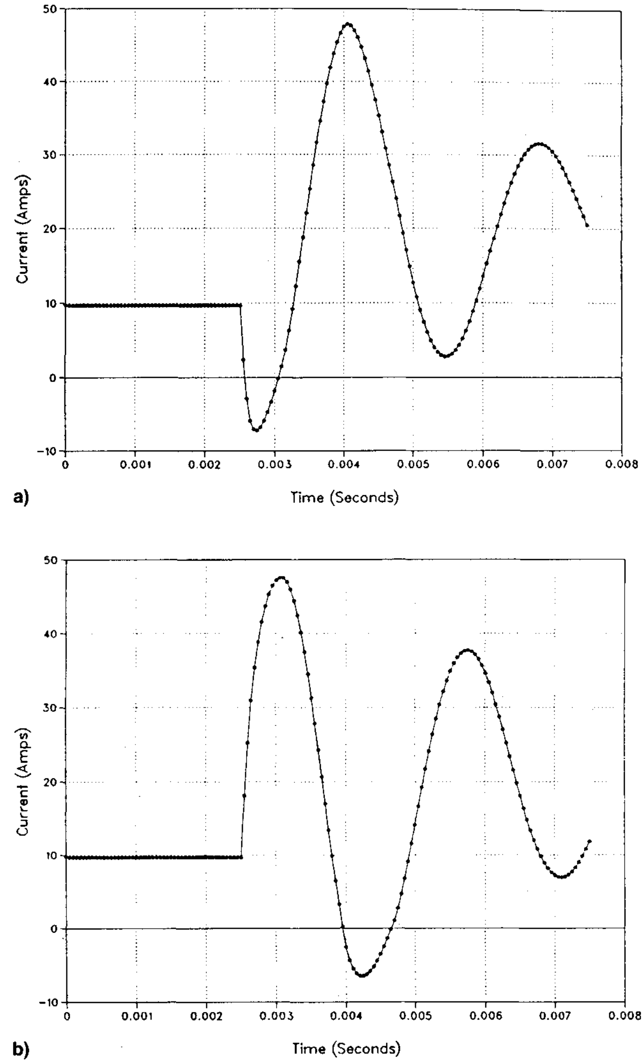

Fig. 5 Field current. Generator no. a) 1 and b) 2.

(3) and the approach and inductance data corresponding to 10-kVA load conditions. In addition, the change from the case of two separate generator systems ($0 \leq t \leq 2.5$ ms) to a system of two generators ($2.5 \leq t \leq 7.5$ ms) was implemented by adjusting the load resistance values in Eq. (3). Furthermore, the value of the voltage across the main field of a generator is computed as the product of the field current and the shunt resistance. This is done in order to calculate the reverse voltage at the terminals of the rotating diode bridge rectifier (Fig. 1).

The simulation of the system under these conditions resulted in the current and voltage waveforms throughout the system. A sample of these results is given in Figs. 3–6. Figs. 3a and 3b show the armature phase (a) currents for generators no. 1 and 2, respectively. An inspection of these figures shows a phase shift $\alpha = 60$ deg between the two generators during the first cycle before the onset of the FPT operation. Furthermore, these waveforms show the higher current values resulting in the armature of both generators after the commencement of the FPT operating condition. In addition, the waveforms of the damper bars direct axis current i_{kd} are shown in Fig. 4 as obtained for both generators. As one expects, the damper bars have zero current values during steady-state operation ($0 \leq t \leq 2.5$ ms). This is due to the fact that both the armature mmf and the rotor are rotating at the same speed. However, the onset of the FPT, at the beginning of the second cycle ($t = 2.5$ ms), resulted in nonzero values for the damper bar currents. This is attributed to the unbalanced operation

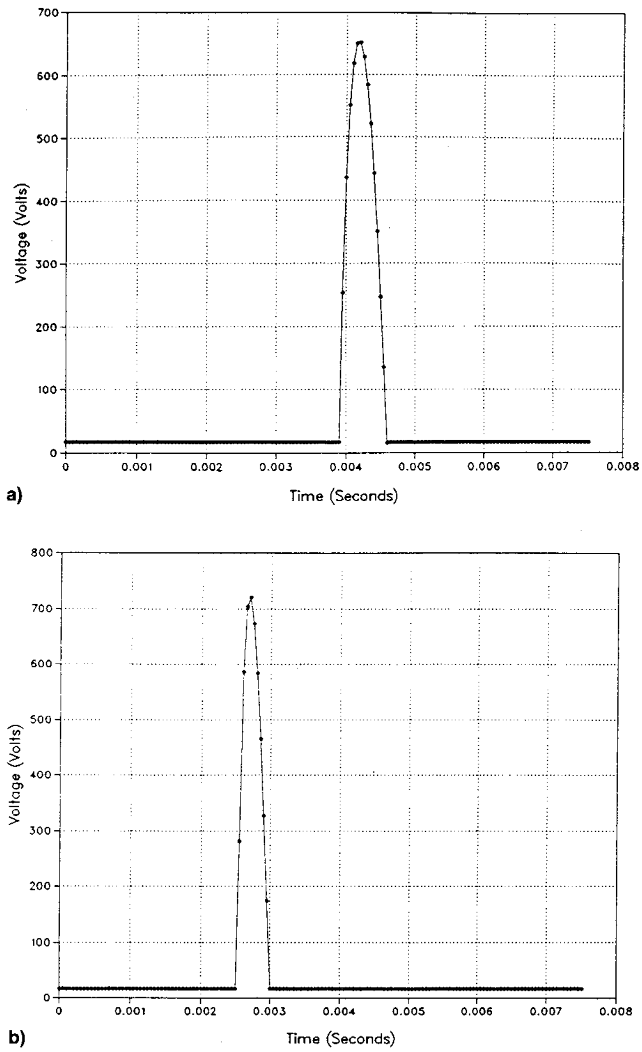

Fig. 6 Reverse field voltage. Generator no. a) 1 and b) 2.

resulting from the FPT. This forced paralleling operation results in a stator mmf rotating at a speed different from the rotor synchronous speed. Moreover, a close inspection of the current waveforms (Fig. 5) indicates a constant positive field current for both machines during the first cycle. However, at the beginning of the second cycle, the leading generator field current (generator no. 2) reverses direction. This negative current flows through the shunt field resistor, producing a reverse voltage whose magnitude has a peak negative value of 720 V (Fig. 6a) across the field winding and associated exciter bridge rectifier circuit. Likewise, generator no. 1 field current reverses direction later during the same cycle and results in a reverse voltage of 650 V across the rectifier bridge of generator no. 1 (Fig. 6b).

A summary of results is given in Table 1. As shown by the results in Table 1 excellent agreement exists between the computed and measured values for α = 60 deg. Next, the analysis was repeated for the same load condition over a set of α, covering a range $20 \leq \alpha \leq 100$ deg. Again, the 10-kVA inductance expressions were used in the analysis. This resulted in all the current and voltage waveforms throughout the system. A summary of results for the magnitude of the peak value of reverse field voltage of generator no. 2 is given in Fig. 7 and Table 2 as obtained from simulations and measurements.

Table 1 Field reverse voltage for α = 60 deg

Generator	Computed	Measured
No. 1	650 V	——
No. 2	720 V	740 V

Table 2 Maximum field reverse voltage

	Computed	Measured
Maximum voltage	753 V	760 V
Phase angle	50 deg	90 deg

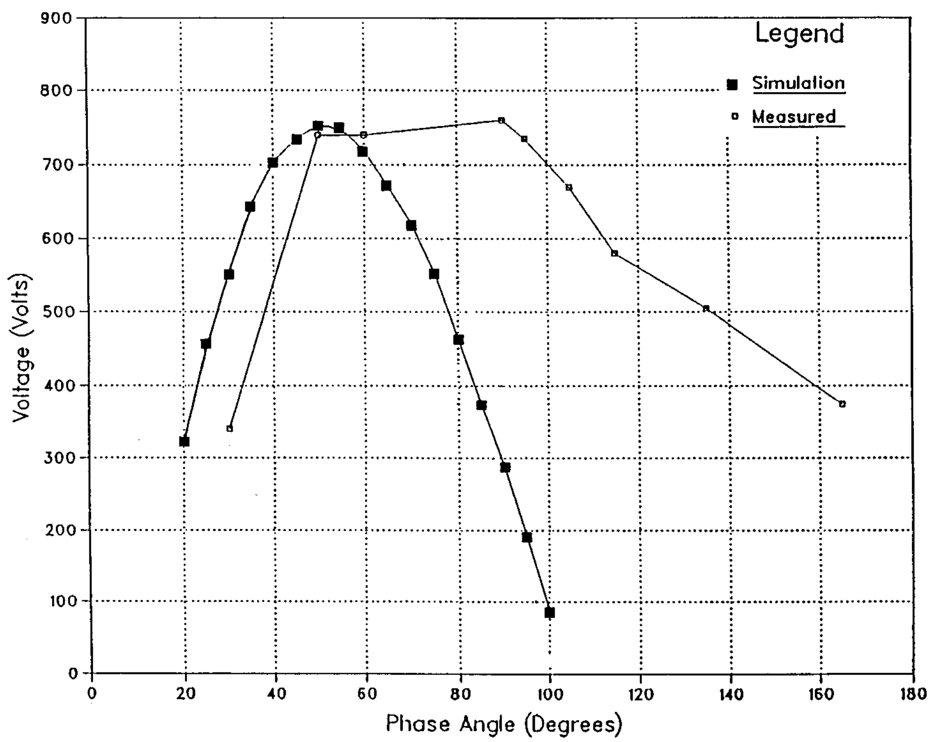

Fig. 7 Maximum reverse field voltage vs α for generator no. 2.

Based on the simulation results a value of 753 V was determined for the magnitude of the maximum reverse field voltage at $\alpha = 50$ deg. Meanwhile, a maximum peak reverse voltage of 760 V was determined from measurements at $\alpha = 90$ deg. An inspection of the results given in Table 2 shows the good agreement for the magnitude of the maximum field reverse voltage as obtained from measurements and simulations. However, it is clear that these maximum values are occurring at different α. This difference can be attributed to the fact that this approach involves the use of nonlinear magnetostatic field solutions that are determined for a given load condition. An improvement on this approach is to extend the finite element algorithm to include the ability to update the inductance values during the simulation period. This can be performed by integrating the state–space model and the finite element model using an iterative approach that allows for the updating of the inductances at each time step of the simulation period based on the instantaneous values of the machine currents. However, the use of such an iterative approach is computationally expensive and would be impractical if it is to be implemented with a multimachine system. Another possible improvement to this approach would be the inclusion of eddy currents due to varying magnetic fields in the finite element model. These eddy currents, resulting from transient disturbances such as FPT, might need to be determined in the different parts of the generator. Finally, it should be stated that in spite of the difference between the predicted and measured values of the phase angle at which the maximum reverse field voltage occurs, it is demonstrated that this modeling approach is effective in determining the maximum reverse voltage that is essential for the proper rating of the diodes in the rotating rectifier bridge.

Conclusions

The results of a case study on the effects of FPT on the performance of high-speed ac generator-load systems were presented. The case study involved two 90-kVA, 208-V, and 400-Hz, 4-pole ac generators and associated loads. The method implemented in the case study is based on the use of state–space models in the *abc* frame of reference and nonlinear magnetostatic field solutions to account for space harmonics and saturation effects. Using this approach resulted in the machine windings current and voltage waveforms throughout the system. In addition, this approach resulted in the maximum value of the reverse voltage, across the rotating diode rectifier bridge of the field exciter, which was verified by comparison to test data.

References

[1]Slemon, G. R., and Straughen, A., *Electric Machines*, Addison–Wesley, Reading, MA, 1982.

[2]Del Toro, V., *Electric Power Systems*, Prentice–Hall, Englewood Cliffs, NJ, 1992.

[3]Kulig, T. S., Buckley, G. W., Lambrecht, D., and Liese, M., "A New Approach to Determine Generator Winding and Damper Currents in Case of Internal and External Faults and Abnormal Operation. Part I: Fundamentals," IEEE-PES Winter Meeting, Paper 87 WM 203-3, New Orleans, LA, Feb. 1987.

[4]Arkadan, A. A., Hijazi, T. M., and Demerdash, N. A., "Computer-Aided Modeling of a Rectified DC Load Permanent Magnet Generator System with Multiple Damper Windings in the Natural abc Frame of Reference," *IEEE Transactions on Energy Conversion*, Vol. 4, No. 3, 1989, pp. 518–525.

[5]Park, R. H., "Two Reaction Theory of Synchronous Machines—Generalized Method of Analysis—Part I," *American Institute of Electrical Engineers Transactions*, Vol. 48, July 1929, pp. 716–727.

[6]"Test Procedures for Synchronous Machines," IEEE Std. 115-1983, Inst. of Electrical and Electronics Engineers, New York, 1983.

[7]Arkadan, A. A., and Kielgas, B. W., "Effects of Force Fitting on the Inductance Profile of a Switched Reluctance Motor," *IEEE Transactions on Magnetics*, Vol. 29, No. 2, 1993, pp. 2006–2009.